Journal of Renewable Energy and Sustainable Development (RESD)
Volume 12, Issue 1, June 2026 - ISSN 2356-8569
http://dx.doi.org/10.21622/RESD.2026.12.1.2100

Received: 25 April 2026 Accepted: 08 June 2026 Published: 28 June 2026

Enhancing Hydropower Sustainability through Air Injection: Experimental Reduction of Sediment Erosion in Francis Turbine Guide Vanes

Prashant Dhiman [1], Abhiraj Chaudhary [2], Nitesh Rautela [3], and Ashish Karn [4*]

[1,3,4*] UPES, School of Advanced Engineering, Mechanical Cluster, Multiphase Flow Laboratory, Dehradun, Uttarakhand, India

[2] Step by Step School, Noida, Uttar Pradesh (UP), India

pdkuk597@gmail.com, pkuk597@gmail.com, niteesh.rautela@ddn.upes.ac.in, ashish.karn@alumni.iitd.ac.in

Abstract

Hydropower is a reliable and renewable source of energy, but plants operating in sediment-laden rivers, particularly in Himalayan regions, frequently experience severe erosive wear of turbine components. Sediment-induced material degradation of guide vanes, runner blades, and other flow-controlling parts increases maintenance frequency, downtime, and lifecycle cost. This study experimentally investigates air injection as a mitigation technique for improving hydropower sustainability through the reduction of sediment erosion in Francis turbine guide vanes. Experiments were performed using a specially developed rotary disc apparatus with guide vane specimens based on the NACA 4412 profile. The effects of sediment concentration (60,000, 80,000, and 100,000 ppm), angle of attack (0°, 15°, and 30°), and air flow rate were systematically evaluated. Results show that air injection significantly decreases material loss compared with non-aerated conditions, with erosion reduction ranging from 32% to 51%. Higher air flow rates provided greater protection, indicating that the injected air forms an effective buffer layer that reduces particle-surface interaction. The findings demonstrate that air injection can enhance component service life, lower maintenance demand, and support more sustainable operation of sediment-prone hydropower plants.

Graphical abstract

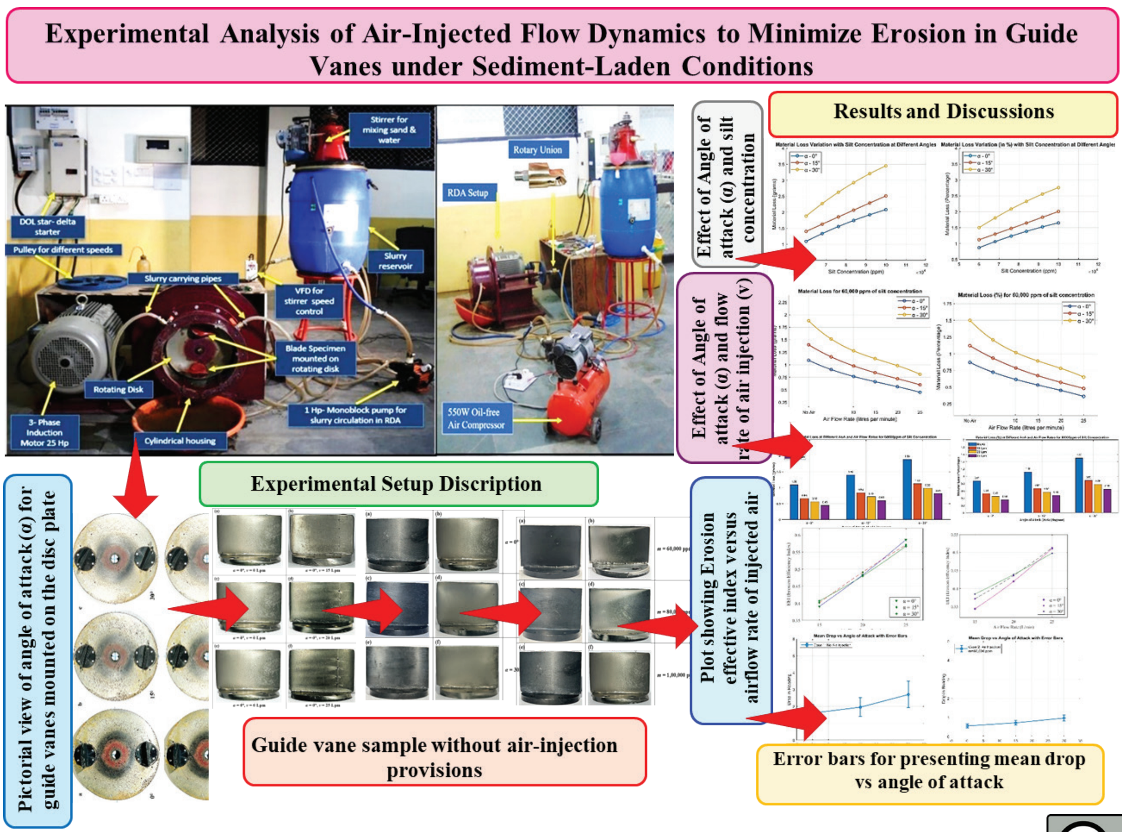

* Corresponding author

Index-words: *Sediment Erosion, Rotary Disc Apparatus (RDA), Guide Vanes, Downtime, Air-injection.*

I. Nomenclature

Details of symbols	
Term	Meaning
α	Angle of attack of hydrofoil (in degrees)
d	Angle of air injection (in degrees)
m	Sediment concentration in the water stream (in parts per million, ppm)
v	Air injection velocity (in Liters per minute, Lpm)

Abbreviations	
Term	Meaning
HVFS	High-Velocity Flame Spraying
HVOF	High-Velocity Oxygen Fuel
NACA	National Advisory Committee for Aeronautics
RDA	Rotary Disc Apparatus
SMAW	Shielded Metal Arc Welding

II. Introduction

Hydropower remains one of the most reliable and mature renewable energy technologies for large-scale electricity generation because of its high conversion efficiency, operational flexibility, and comparatively low running cost. In addition to electricity production, hydropower infrastructure contributes to irrigation support, flood moderation, water management, navigation, tourism, and regional socio-economic development, thereby strengthening its role in sustainable energy systems [1]. Despite these advantages, long-term operation of hydropower plants is frequently constrained by component degradation mechanisms such as cavitation, fatigue, structural damage, and sediment-induced wear, all of which reduce plant availability and increase maintenance demand [2].

Among these challenges, sediment erosion is particularly severe in plants operating on rivers carrying high suspended solid loads. This issue is especially relevant in Himalayan catchments, where glacial activity, landslides, monsoon runoff, and young geological formations generate large quantities of abrasive particles. When such sediment-laden water passes through hydraulic machinery, repeated particle impacts and sliding interactions progressively remove material from critical components such as guide vanes, runner blades, needles, nozzles, and casing surfaces. The resulting wear lowers hydraulic performance, increases vibration risk, shortens service life, and leads to costly shutdowns for repair or replacement [3]. The erosion process depends on several interacting variables, including particle concentration, size, hardness, morphology, impact angle, local flow velocity, material properties, and surface condition of the exposed component [4], [5].

One of the most established approaches is upstream sediment management through settling basins, desilting chambers, and hydraulic exclusion systems that remove coarse particles before water enters the turbine. Previous studies have emphasized the importance of properly designed desilting facilities for improving operational reliability and reducing hydro-abrasive damage [6], [7], [8].

Another important line of defense is real-time sediment monitoring and adaptive operation. Modern instrumentation, such as optical backscatter sensors, laser diffraction systems, acoustic techniques, turbidimeters, and LISST-based devices, enables continuous estimation of suspended sediment concentration and particle characteristics. These systems help operators modify loading schedules, shut down units during extreme events, or optimize maintenance planning before severe damage occurs [9], [10], [11], [12].

Surface engineering has also been extensively investigated to improve the erosion resistance of turbine materials. Protective coatings based on nickel-, chromium-, carbide-, and cobalt-rich systems have been applied to vulnerable surfaces to enhance hardness, toughness, and resistance to particle impact. Reported performance depends strongly on coating microstructure, porosity, bonding quality, residual stress state, and deposition route [13], [14]. Various manufacturing and repair processes, including shielded metal arc welding, flame spraying, plasma spraying, microwave cladding, and high velocity oxygen fuel techniques, have been examined for hydroturbine applications [15], [16], [17], [18], [19]. While coatings can substantially delay wear, they increase maintenance complexity and cost, and coating failure may still occur under aggressive sediment conditions.

In parallel with these approaches, aeration and air injection have been successfully employed in several hydraulic engineering applications. Air admission has been used to improve dissolved oxygen levels in downstream water bodies, enhance environmental performance, and modify undesirable flow structures such as vortices in hydroturbine draft tubes and related systems [20], [21], [22]. Air entrainment has also been studied as a means of mitigating cavitation damage, where injected bubbles alter pressure fluctuations, cushion collapse events, and modify near-wall flow behavior in tunnels and hydrofoils [23], [24], [25], [26], [27]. These findings suggest that controlled gas-liquid interaction can be used not only for environmental or cavitation control purposes, but also for protecting solid surfaces exposed to aggressive hydraulic conditions. Along with gas, oil-based experiments were also performed by researchers, which reveal that the performance of turbines can be improved and also highlight that preheating oil shows better performance of axial-flow turbines [28].

More recently, air injection has emerged as a potential strategy for reducing sediment erosion. Preliminary studies proposed that injected air will possibly form a layer or dispersed bubble field near the surface, which may reduce direct particle-wall collisions of the sediment particles in the silt-laden water, decrease momentum transfer, and alter particle trajectories in a favorable manner [29]. Later, subsequent numerical and experimental investigations supported the possibility of such a buffer layer by measurable erosion reduction under multiphase flow conditions representative of hydraulic machinery [30]. Early experimental evidence further indicated that aeration can lower material loss under sediment-laden operating environments [31]. However, prior studies have presented air-injection as a technique for mitigating or reducing sediment erosion and provided preliminary reports regarding the efficacy of this technique.

Guide vanes are of particular interest because they are among the first major flow-controlling components exposed to sediment-laden water in Francis turbines. Their dual role in regulating discharge and directing flow toward the runner makes their integrity essential for both efficiency and reliable operation. Excessive wear of guide vanes can distort flow guidance, increase leakage, and accelerate downstream damage. Therefore, the development of practical methods to reduce guide vane erosion can provide system-wide benefits in performance, maintenance planning, and lifecycle cost.

In this context, the present study, based on those findings, experimentally investigates the air injection technique under a broader range of operating conditions to develop a comprehensive understanding of the performance and efficacy of the proposed air-injection technique. Experiments were conducted using a specially developed rotary disc apparatus equipped with guide vane specimens based on the NACA 4412 profile. The effects of sediment concentration (60,000, 80,000, and 100,000 ppm), angle of attack (0°, 15°, and 30°), and air flow rate (15, 20, and 25 L/min) were systematically evaluated. The objective is to quantify the extent to which controlled air injection reduces material loss and to assess its potential as a practical strategy for extending component life, reducing maintenance burden, and improving long-term hydropower reliability.

III. Material & Methods

A. Guide vane samples

Guide vanes were selected as the test component because they are among the first hydraulic elements in a Francis turbine to encounter sediment-laden flow and are therefore highly susceptible to hydro-abrasive wear during operation [32], [33]. In addition to their exposure to incoming particles, guide vanes play a critical role in regulating discharge and directing flow toward the runner, making their surface integrity important for both efficiency and operational reliability.

The test specimens used in the present work were manufactured using the NACA 4412 hydrofoil profile, as shown in Figure 1(a) and Figure 1(b). This profile was selected based on earlier investigations reporting comparatively favorable behavior under sediment-laden conditions, including lower erosion tendency, reduced pressure-side to suction-side pressure differential, and lower overall material loss relative to alternative guide vane profiles [34]. The use of a standardized hydrofoil geometry also improves repeatability and allows meaningful comparison with previously reported studies.

B. Material properties and surface preparation

Hydroturbine components are commonly fabricated from turbine steels and other wear-resistant metallic alloys because of their mechanical strength and durability in hydraulic service environments [35]. However, aluminum alloy specimens were employed in the present experimental investigation. Because it has comparatively lower hardness, it accelerates measurable wear within practical test durations, thereby reducing experimental time while preserving the relative trends associated with changing operating conditions. Further, a similar study using aluminum alloy runner blade specimens was conducted by Rajkarnikar et al. (2013), who employed aluminum as a representative for lab-scale erosion experiments. The study presented wear characteristics and erosion patterns compared to those observed in hydro-turbine components, supporting the use of aluminum alloy material for calculating the effect of different operating parameters and sediment-erosion mitigating techniques. In addition, aluminum alloys are cost-effective, easy to machine, and convenient for specimen preparation, which makes them suitable for comparative erosion studies and rapid screening of mitigation techniques [36].

The guide vane specimens were first cast to the required geometry and subsequently joined to supporting plates. Then, the surfaces of the specimens were mechanically polished to remove oxide layers, residual surface irregularities, and manufacturing defects. The primary response variable in this study was total material loss; the preparation procedure focused on consistency of the initial surface state rather than optimization of roughness as an independent parameter. To facilitate post-test visual examination of worn regions and erosion patterns, the polished specimens were anodized with a black surface layer prior to experimentation. This coating served only as a visual contrast layer to highlight zones of material removal after testing. It was not intended as a protective coating and was not considered to contribute to erosion resistance. Differences observed after testing were therefore attributed to the interaction between the sediment-laden flow, the specimen material, and the applied air-injection conditions.

IV. Experimental design & Parameters

A full factorial Design of Experiments (DoE) methodology was adopted to systematically evaluate the influence of selected operating parameters on sediment erosion of guide vane specimens under sediment-laden flow conditions.

Three independent variables were considered, and each variable was examined at three levels, resulting in a 3^3 full factorial design comprising 27 unique operating conditions. The selected design enables estimation of main effects as well as interaction effects between variables, which is particularly important when the erosion response is sensitive to coupled changes in sediment loading, vane orientation, and air injection intensity. Compared with one-factor-at-a-time testing, a full factorial design provides higher information content, improved statistical interpretability, and a more rigorous basis for identifying trends in complex engineering systems [37], [38].

The factorial matrix constituted the primary test plan for air-injection cases. In addition, corresponding baseline experiments without air injection were performed for comparison under the same sediment concentration and angle of attack conditions. This combined approach allowed direct quantification of the mitigation benefit achieved through aeration.

Hydro-abrasive erosion is affected by numerous interrelated variables, including particle size, particle shape, surface texture, mineral hardness, target material properties, impact angle, local flow velocity, turbulence intensity, and sediment concentration [32], [39], [40], [41]. Since simultaneous variation of all such parameters is impractical in laboratory-scale experimentation, the present study focused on a reduced set of dominant and controllable variables directly relevant to the proposed mitigation technique. The selected independent variables were: Angle of attack of the guide vane, α; Sediment concentration in the water stream, m and; Air flow rate for injection, v.

These variables were chosen because they represent, respectively, the hydraulic loading condition of the guide vane, the severity of erosive particle exposure, and the strength of the protective

Volume 12, Issue 1, June 2026 - ISSN 2356-8569
http://dx.doi.org/10.21622/RESD.2026.12.1.2100

air layer introduced at the surface. The fixed operating conditions and variable test levels used in the present investigation are summarized in Table 1.

Table 1: Description of parameters.

Sr. No.	Fixed Parameters		Variable Parameters	
1.	Speed of the Disc plate	720 rpm	Angle of attack (α)	0°, 15° and 30°
2.	Operating Time	400 minutes	Sediment Concentration (m)	60,000 ppm, 80,000 ppm, and 1,00,000 ppm
3.	Sediment Size	0-200 µm	Flow rates of air injection (v)	15 Lpm, 20 Lpm, and 25 Lpm

The selected ranges were considered appropriate for accelerated laboratory evaluation of erosion and for comparing the effectiveness of air injection under progressively severe operating conditions. Maintaining fixed values of rotational speed (720 rpm), operating time (400 minutes), and particle size (200 um) ensured that the measured differences in material loss could be primarily attributed to the chosen independent variables. Additional geometric and operational characteristics of the experimental setup are provided in Table 2.

Table 2: Geometrical and operational characteristics of the test rig.

Sr. No.	Characteristics	Value
1.	Speed of the disc plate	720 rpm
2.	Diameter of the disc	390 mm
3.	Guide Vane Profile	NACA 4412
4.	Means of air-injection	Holes on the pressure side
5.	Size of holes	1 mm in diameter
6.	Angle of air-injection	~ 50°

The air injection geometry was designed to introduce air near the guide vane surface in a controlled manner so that the resulting gas-liquid interaction could influence particle trajectories and reduce direct particle-wall contact. Together, the selected parameters and apparatus configuration provide a consistent basis for evaluating air injection as a sediment erosion mitigation strategy for Francis turbine guide vanes.

V. Experimental setup

A. Equipment description

The experimental investigation was carried out using a specially developed laboratory-scale erosion test rig designed to reproduce the principal hydrodynamic conditions associated with sediment-laden flow in hydropower systems. The rig configuration was conceptually based on a previously reported rotating disc apparatus used for hydro-abrasive erosion studies, while being modified to accommodate controlled air-injection experiments on guide vane specimens [36].

The facility was developed to enable accelerated testing of scaled guide vane and runner-type components under repeatable laboratory conditions, thereby reducing the time required to obtain comparative erosion data. A schematic representation of the setup is shown in Figure 1(c).

The core of the system consists of a rotating shaft connected to a circular disc plate driven by a three-phase induction motor. The motor supplied the torque necessary to maintain the prescribed rotational speed under combined hydraulic drag and mechanical loading during operation. Test specimens were securely mounted on the rotating disc so that their surfaces remained exposed to the sediment-laden working fluid throughout the experimental cycle. The rotating assembly was enclosed within a cylindrical casing chamber to safely contain the multiphase flow environment.

A dedicated pump circulated the sediment-water mixture into the test chamber. To maintain homogeneous suspension of solid particles and avoid settling in the supply tank, a separate mechanically driven stirrer was installed in the mixing reservoir. Continuous agitation was essential to ensure that the sediment concentration remained as uniform as possible during each test run. The stirrer speed was regulated using a Variable Frequency Drive (VFD), allowing controlled operation of the mixing system.

For air-injection cases, an oil-free air compressor supplied compressed air to the guide vane specimens through the designated injection passages. The delivered air flow rate was adjusted and monitored using a calibrated airflow meter before entering the test section. This arrangement enabled systematic variation of aeration intensity while maintaining identical hydraulic and sediment conditions for comparative analysis.

The complete setup also included connecting pipelines, valves, hoses, sealing elements, electrical controls, mounting fixtures, and measuring instruments required for safe and reliable operation. The integrated design provided a controlled platform for evaluating the effectiveness of air injection in mitigating sediment erosion of Francis turbine guide vanes.

(a)

(b)

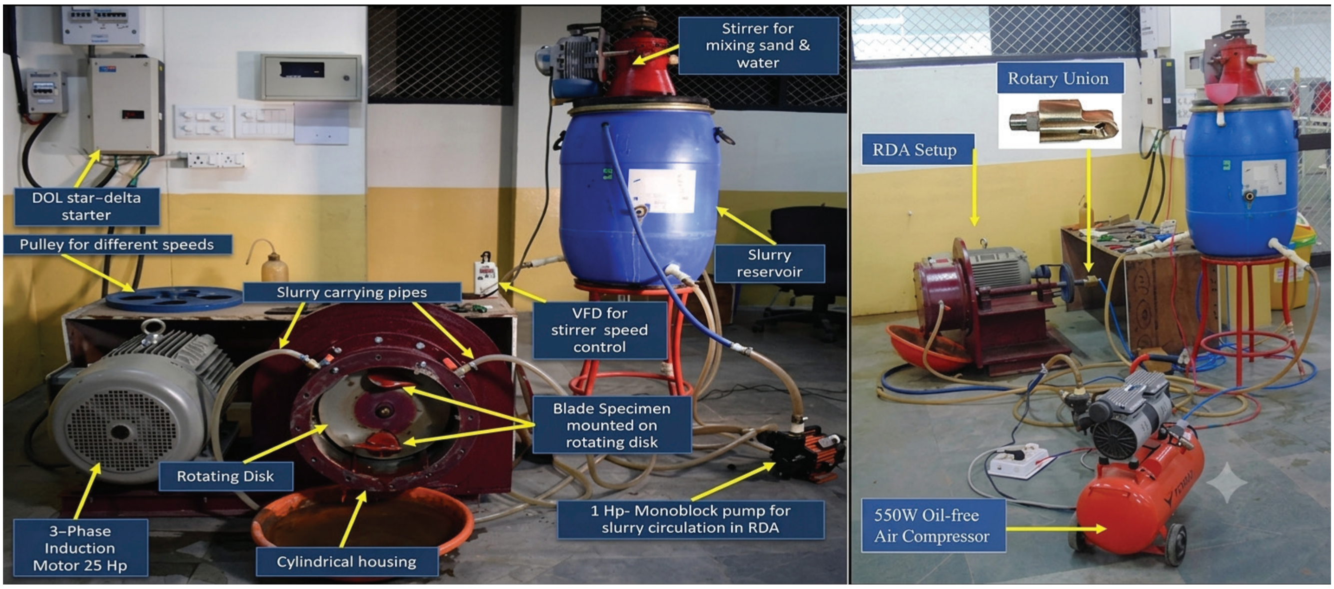

(c)

Figure 1: (a) Guide vane sample without air-injection provisions, (b) Guide vane sample with air-injection provisions, and (c) Description of setup with its different components.

Repeatability and experimental consistency were carefully maintained throughout the investigation. Prior to each test series, all measuring instruments, including the airflow meter, tachometer, and weighing balance, were inspected and calibrated according to standard reference procedures to ensure measurement reliability. Preliminary trial experiments were also conducted to validate the performance and accuracy of the experimental setup and measuring equipment. The weighing balance used in the experiments had a resolution of ±0.01 g, providing sufficient precision for the measurement of material loss. The uncertainty analysis revealed relatively low uncertainties for most measured parameters, generally below 0.13%. However, the uncertainty associated with the angle of attack was comparatively higher, approximately 5%, primarily due to limitations in the settling and alignment mechanism. The repeatability of the experimental apparatus was further assessed through repeated primary trial experiments. The measured material loss exhibited a mean value of 1.346 g with a standard deviation of 0.2021 g, indicating acceptable experimental consistency and satisfactory repeatability of the test setup. In fact, the observed repeatability exceeded 85%, indicating satisfactory reliability of the experimental methodology for comparative assessment of material loss trends.

Volume 12, Issue 1, June 2026 - ISSN 2356-8569
http://dx.doi.org/10.21622/RESD.2026.12.1.2100

VI. Results & Discussions

The primary objective of this study was to evaluate the ability of controlled air injection to reduce sediment-induced material loss from Francis turbine guide vane surfaces under sediment-laden operating conditions. The experimental program compared baseline non-aerated cases with aerated cases over a range of sediment concentrations, guide vane angles of attack, and air flow rates. Across the tested operating envelope, the results consistently demonstrate that air injection reduces erosive wear, with the magnitude of protection depending on both hydraulic loading and aeration intensity.

For clarity, the results are discussed in four parts: (i) baseline erosion behavior without air injection, (ii) influence of air injection under different sediment concentrations, (iii) visual evidence from specimen surfaces, and (iv) performance metrics and uncertainty analysis.

A. Baseline erosion behavior without air injection

The non-aerated experiments establish the reference condition against which all air-injection cases were evaluated. Figure 2(a) presents the variation of material loss with angle of attack, α, and sediment concentration, m, while Figure 2(b) shows the corresponding percentage material loss.

A clear increase in material loss is observed with increasing angle of attack. For the tested guide vane geometry, larger values of α expose a greater effective surface area to the incoming sediment-laden flow and modify the local impact direction of particles. This increases the frequency and severity of particle-wall interactions, leading to higher erosion rates. In practical turbine operation, the guide vane angle is adjusted according to load demand and discharge regulation. Therefore, although a higher α may be operationally necessary, it can also intensify wear.

Material loss also increases with sediment concentration. As the number of abrasive particles in the working fluid rises, the cumulative impact energy transferred to the surface increases, producing greater mass removal. The data indicate that the increase is not strictly linear over the tested range, suggesting interaction between particle loading, flow structure, and repeated surface damage.

The combined effect of high sediment concentration and high angle of attack produces the most severe erosion. These baseline results confirm the need for practical mitigation strategies for guide vanes operating in sediment-prone hydropower plants. Previous studies have similarly highlighted the vulnerability of hydraulic components under abrasive flow conditions and the need for innovative control methods [29], [30].

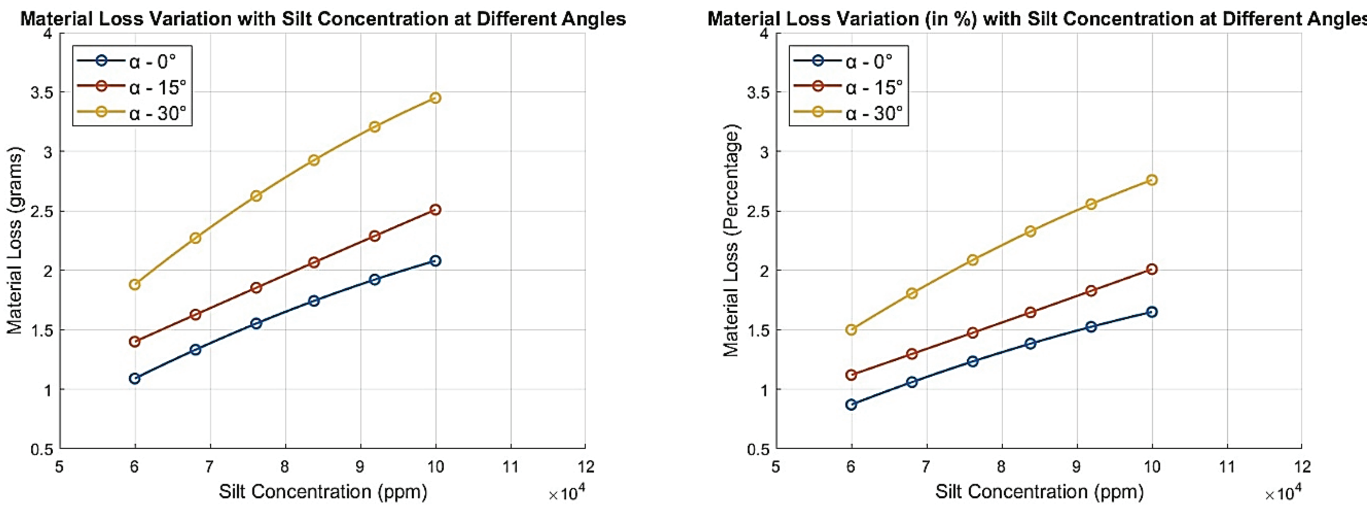

(a) (b)

Figure 2: Effect of angle of attack (α) and silt concentration (m) on (a) material loss and (b) percentage material loss in guide vanes during experiments conducted without air injection.

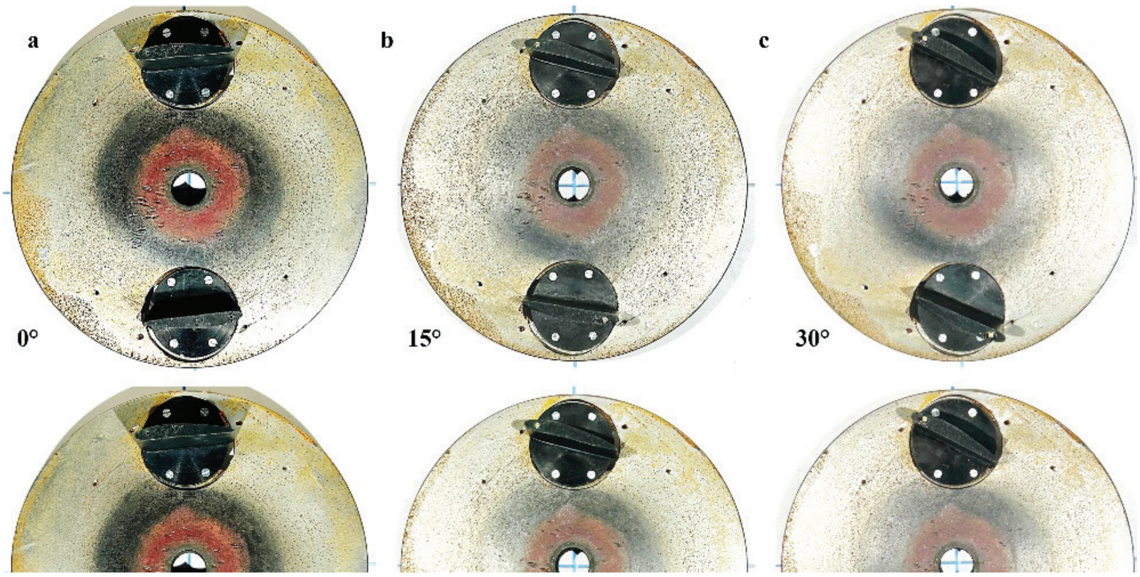

Figure 3: Pictorial view of angle of attack (α) for guide vanes mounted on the disc plate.

The results for different sediment concentrations are discussed separately to highlight the influence of operating severity and to evaluate how airflow rate interacts with vane loading conditions to mitigate erosive wear.

1. Sediment concentration: 60,000 ppm

Figure 4 shows the effect of air flow rate on material loss and percentage material loss at a sediment concentration of 60,000 ppm for α = 0°, 15°, and 30°. For all three guide vane angles, material loss decreases progressively with increasing air flow rate. This monotonic reduction indicates that stronger aeration improves surface protection. The highest wear is observed at α = 30°, followed by 15° and 0°, which is consistent with the baseline trends.

At the most severe condition within this concentration set, the measured material loss decreased from approximately 1.09 g in the non-aerated case to about 0.45 g at 25 L/min air injection, corresponding to nearly 51% reduction. Intermediate air flow rates also produced substantial improvement, confirming that even moderate aeration can suppress erosion.

The observed behavior suggests that injected air acts as a near-wall buffer layer that partially separates abrasive particles from the solid surface and reduces collision intensity.

2. Sediment concentration: 80,000 ppm

The corresponding results for 80,000 ppm sediment concentration are shown in Figure 5. As expected, absolute material loss values are higher than those at 60,000 ppm because of the greater abrasive particle loading. Despite the harsher operating conditions, air injection remains effective across all tested guide vane angles. Increasing the air flow rate continues to reduce material loss relative to the non-aerated baseline. This indicates that the protective mechanism is robust even when sediment concentration increases.

In some cases, the absolute increase in wear with sediment concentration remains noticeable even under aerated conditions. This implies that air injection mitigates erosion but does not fully eliminate the influence of particle loading. The balance between protective bubble coverage and increased turbulence at higher flow intensities may also influence the measured response.

3. Sediment concentration: 100,000 ppm

Figure 6 presents the results for the highest tested sediment concentration of 100,000 ppm. The same general trend is preserved: aerated cases exhibit lower material loss than the corresponding non-aerated cases, and higher air flow rates provide stronger protection.

Volume 12, Issue 1, June 2026 - ISSN 2356-8569
http://dx.doi.org/10.21622/RESD.2026.12.1.2100

Although wear levels remain the highest in absolute terms at this concentration, the persistence of erosion reduction demonstrates that air injection is effective even under severe sediment-laden conditions. This is important from an application perspective because the greatest benefit of mitigation strategies is often required during high-silt operating periods.

Overall, the results from Figures 4-6 confirm three consistent trends:

- Material loss increases with sediment concentration.
- Material loss increases with the angle of attack.
- Material loss decreases with increasing air flow rate.

These trends collectively support the feasibility of air injection as a practical erosion mitigation technique for Francis turbine guide vanes.

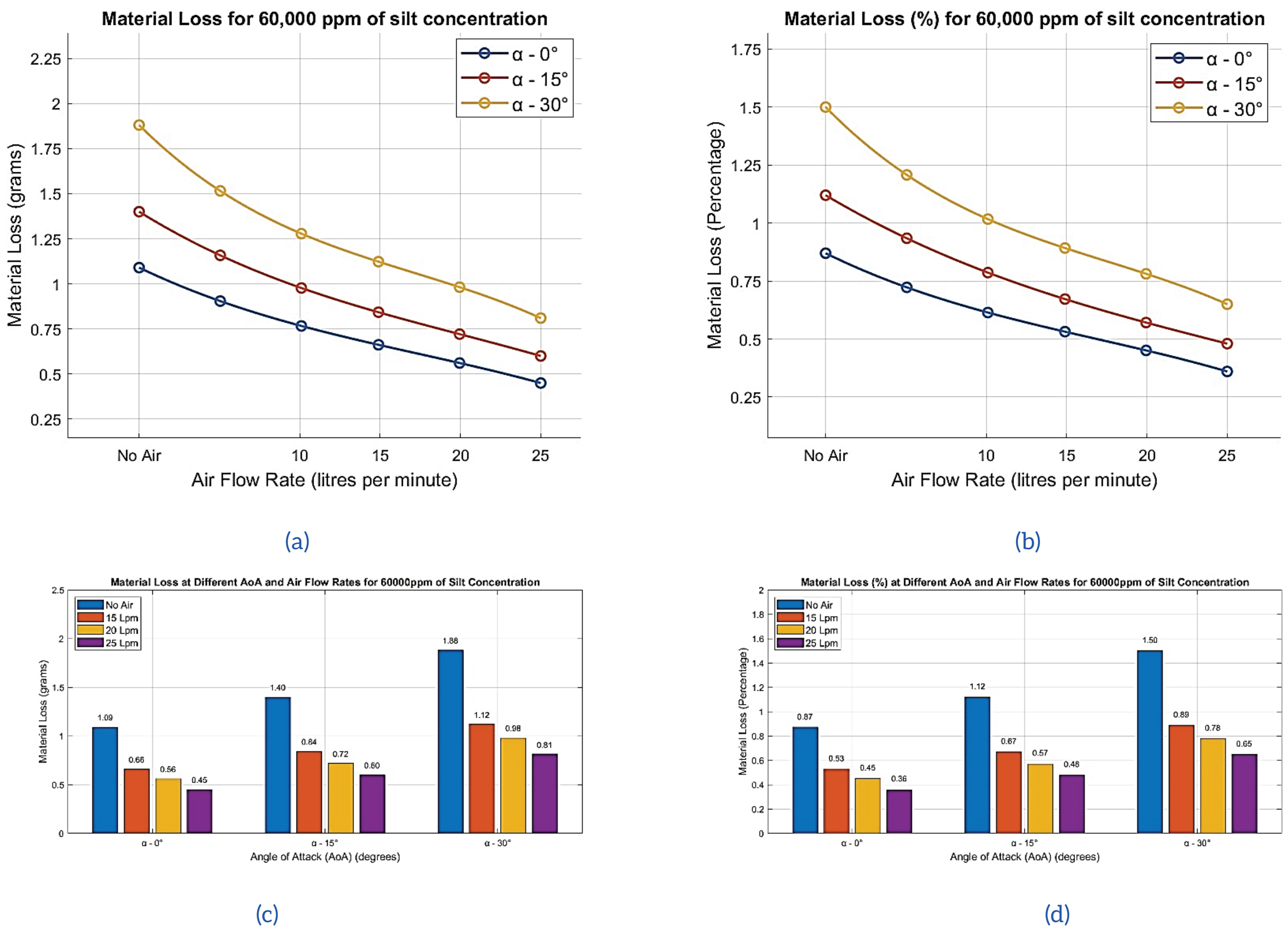

Figure 4: Effect of angle of attack (α) and flow rate of air injection (v) on (a) & (c) material loss and (b) & (d) percentage material loss in guide vanes during experiments conducted without and with air injection for silt concentration of 60,000 ppm.

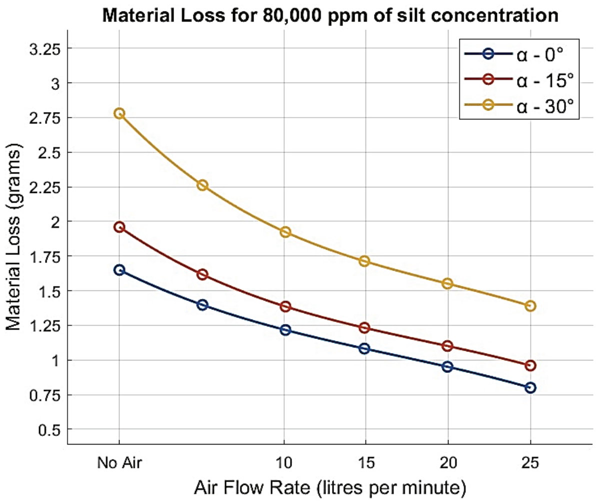

(a)

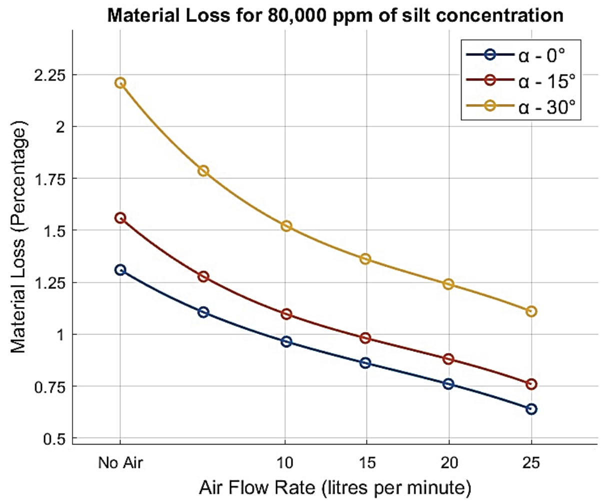

(b)

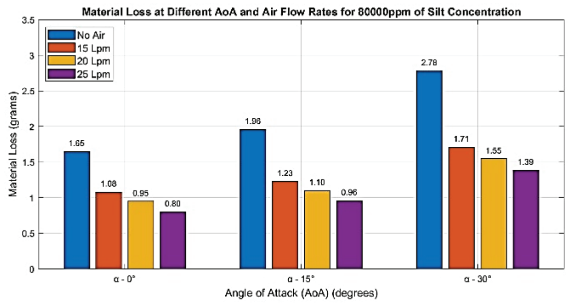

(c)

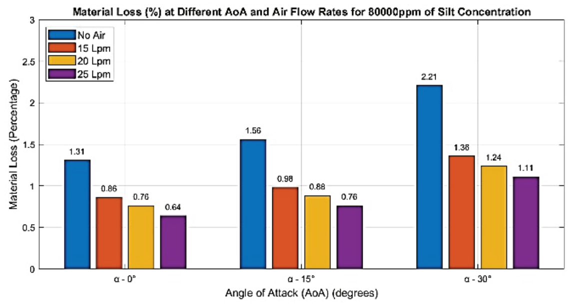

(d)

Figure 5: Effect of angle of attack (α) and flow rate of air injection (v) on (a) & (c) material loss and (b) & (d) percentage material loss in guide vanes during experiments conducted without and with air injection for silt concentration of 80,000 ppm.

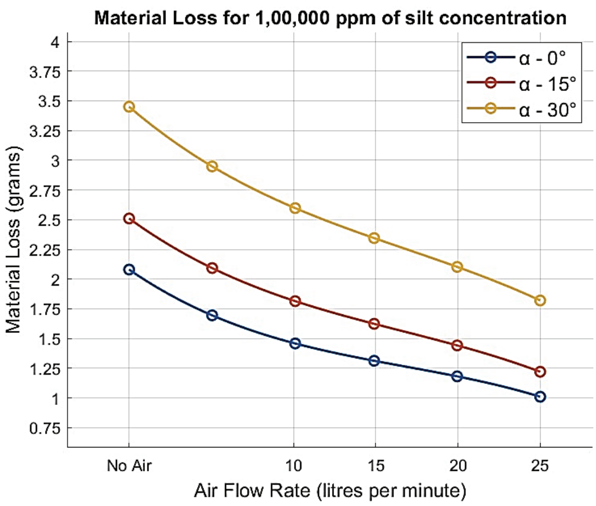

(a)

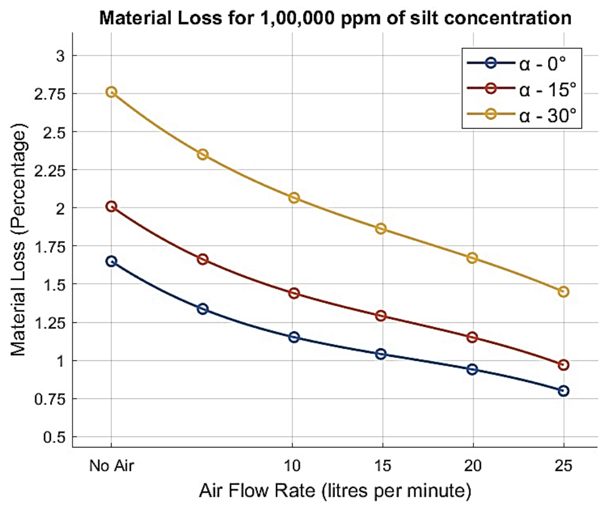

(b)

Volume 12, Issue 1, June 2026 - ISSN 2356-8569
http://dx.doi.org/10.21622/RESD.2026.12.1.2100

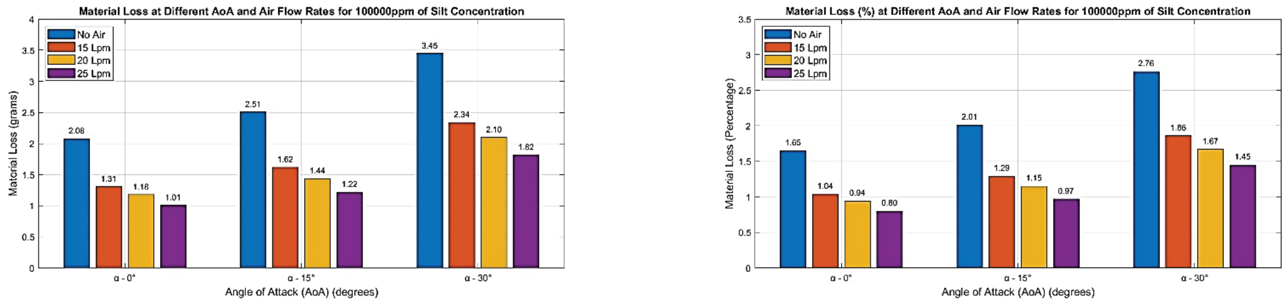

(c) (d)

Figure 6: Effect of angle of attack (α) and flow rate of air injection (v) on (a) & (c) material loss and (b) & (d) percentage material loss in guide vanes during experiments conducted without and with air injection for silt concentration of 1,00,000 ppm.

B. Effect of air injection on material loss

Introduction of air through the guide vane surface significantly reduced material loss relative to the corresponding non-aerated cases. Air was supplied through the pressure-side injection arrangement while the guide vane orientation was varied according to the angle of attack configuration illustrated in Figure 3.

1. Surface morphology and visual evidence

In addition to gravimetric measurements, post-test inspection of the specimens provided direct visual evidence of erosion behavior. Because all samples were coated with a black anodized contrast layer prior to testing, regions of material removal were readily identifiable after exposure.

1. **Effect of angle of attack**
   Table 3 compares specimens tested at different guide vane angles under identical sediment concentration and operating conditions. As α increases from 0° to 30°, progressively larger portions of the contrast layer are removed, indicating more severe wear.

   At lower angles, erosion is concentrated near the leading edge and selected downstream regions. At higher angles, the damaged area becomes broader and more uniformly distributed over the exposed surface. These observations are consistent with the measured increase in material loss shown in Figure 2.

2. **Effect of sediment concentration**
   Table 4 compares specimens tested at increasing sediment concentration for α = 0° without air injection. Surface damage intensifies as sediment loading increases from 60,000 to 100,000 ppm. The gradual disappearance of the black contrast layer confirms that greater particle concentration leads to higher cumulative wear, in agreement with the gravimetric data.

3. **Effect of air injection**
   Table 5 compares non-aerated and aerated specimens at identical operating conditions for different air flow rates. Clear retention of the contrast layer is observed in the air-injected cases, confirming reduced surface damage. Furthermore, the degree of retained surface coverage increases as the air flow rate rises from 15 to 25 L/min. This visual trend supports the quantitative finding that stronger aeration provides better erosion protection.

Volume 12, Issue 1, June 2026 - ISSN 2356-8569
http://dx.doi.org/10.21622/RESD.2026.12.1.2100

Table 3: Visual comparison of the guide vane samples before and after one complete cycle of 400 minutes for different angles of attack (α) at 1,00,000 ppm value of sediment concentration.

(a) 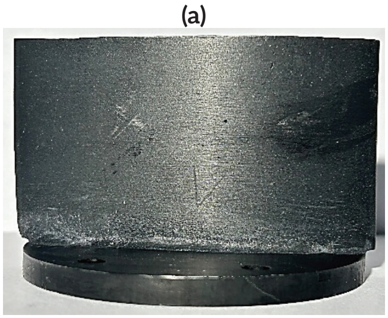	(b) 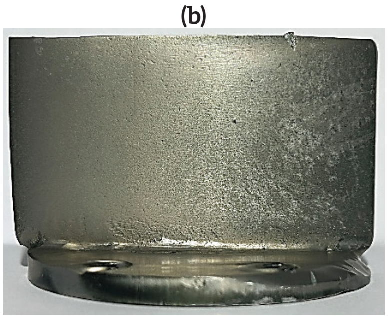	$\alpha = 0°$
(c) 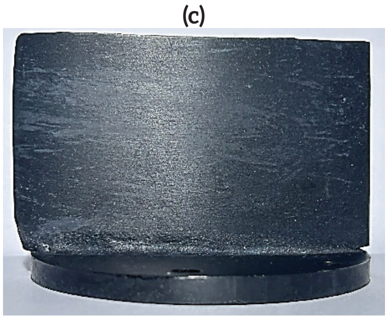	(d) 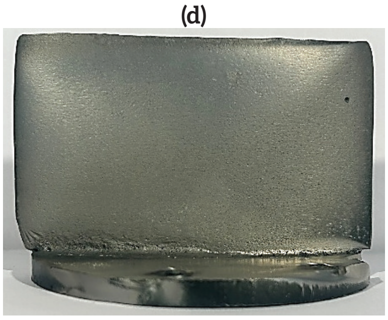	$\alpha = 15°$
(e) 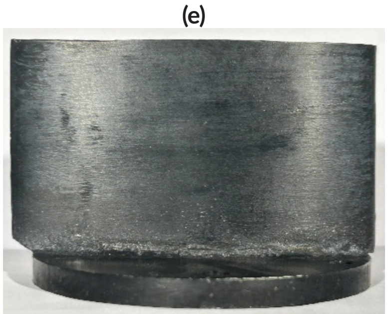	(f) 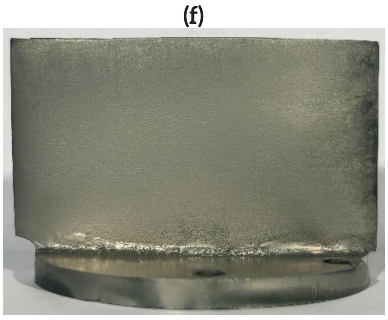	$\alpha = 30°$

Table 4: Visual comparison of the guide vane samples before and after one complete cycle of 400 minutes for different values of sediment concentration (m) for $\alpha = 0°$.

(a) 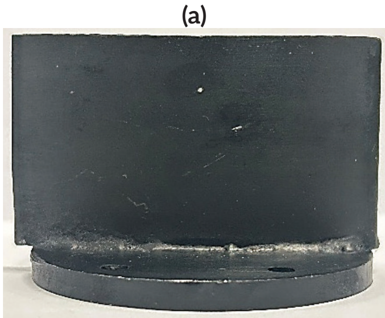	(b) 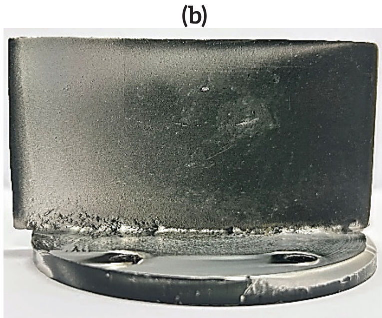	m = 60,000 ppm
(c) 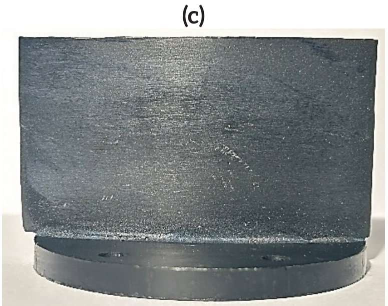	(d) 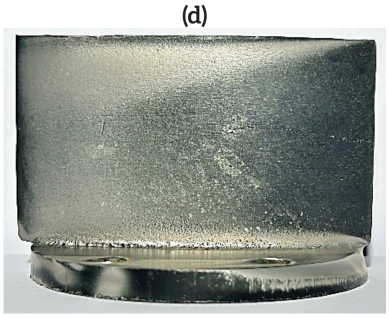	m = 80,000 ppm

Volume 12, Issue 1, June 2026 - ISSN 2356-8569
http://dx.doi.org/10.21622/RESD.2026.12.1.2100

(e) 	(f) 	***m*** = 1,00,000 ppm

Table 5: Visual comparison of the guide vane samples without and with air-injection after one complete cycle of 400 minutes for different values of air flow volume (v) for sediment content of 1,00,000 ppm and α = 0°.

(a)  α = 0°, v = 0 Lpm	(b)  α = 0°, v = 15 Lpm
(c)  α = 0°, v = 0 Lpm	(d) 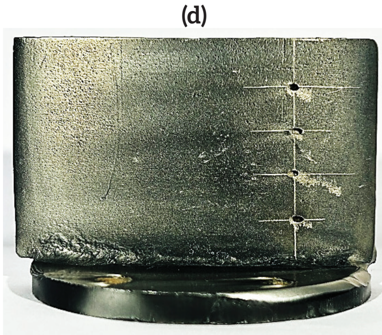 α = 0°, v = 20 Lpm
(e)  α = 0°, v = 0 Lpm	(f) 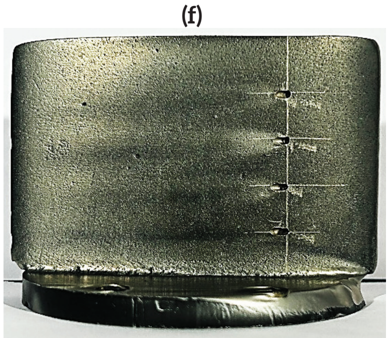 α = 0°, v = 25 Lpm

C. *Erosion Efficiency Index (EEI)*

To provide an additional comparative metric, an Erosion Efficiency Index (EEI) was introduced:

$$EEI = 1 - \frac{Percent\ material\ loss\ (with\ air - injection)}{Percent\ material\ loss\ (without\ air - injection)} \quad (1)$$

This dimensionless parameter expresses the relative reduction in erosion achieved through air injection compared with the corresponding baseline case. Higher EEI values indicate greater mitigation effectiveness.

Figure 7 presents EEI as a function of air flow rate for the three sediment concentrations and all tested angles of attack. In general, EEI increases with air flow rate, demonstrating that stronger aeration improves protection. The index also provides a convenient means of comparing performance across different operating conditions where absolute material loss values differ.

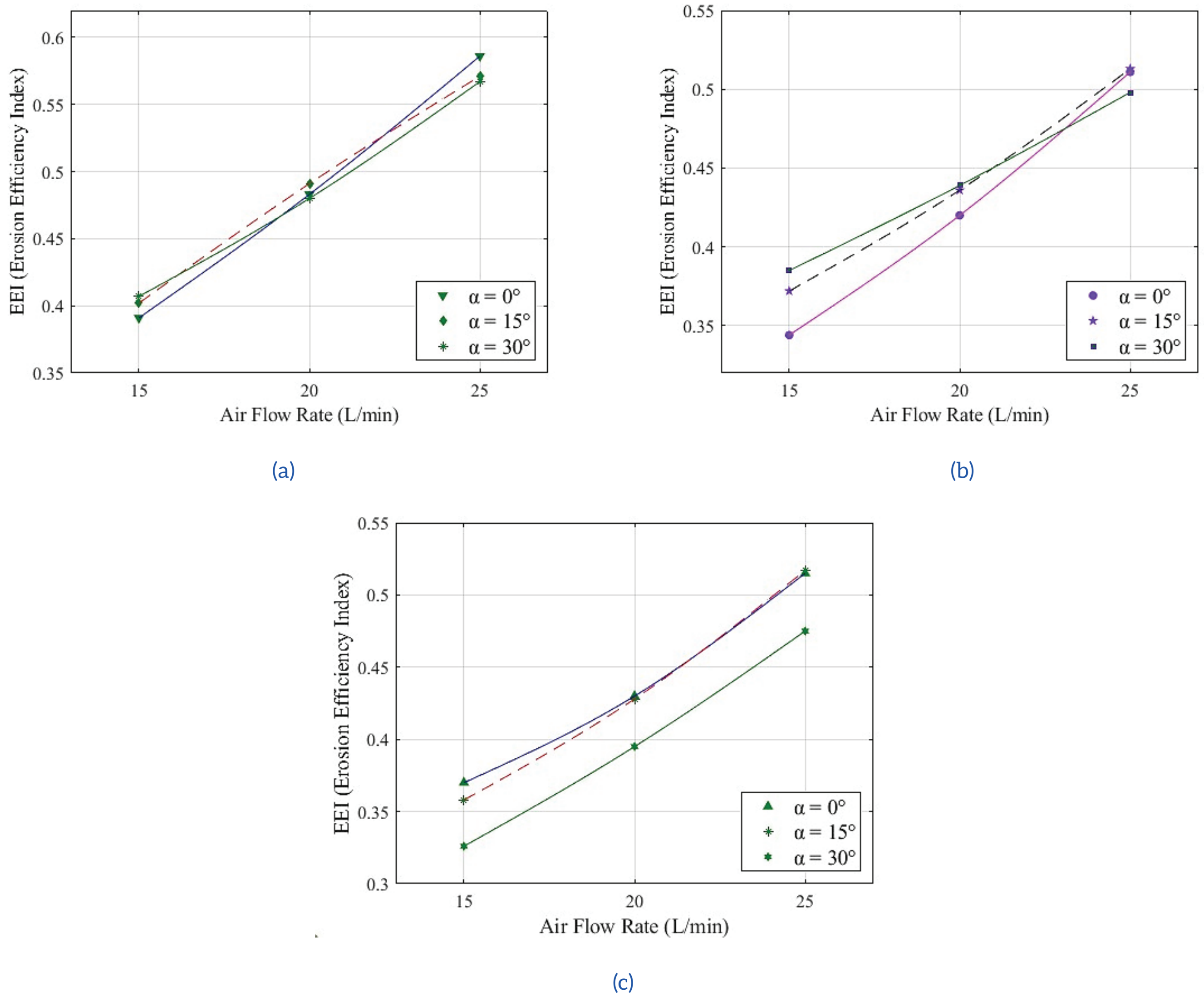

Figure 7: Plot showing Erosion effective index versus airflow rate of injected air for (a) 60,000 ppm, (b) 80,000 ppm, and (c) 1,00,000 ppm of sediment concentration.

D. Calculations, uncertainty, and error analysis

Based on the experimental observations and subsequent statistical analysis, the coefficient of determination (R^2) obtained for the regression model is 0.9344, while the corresponding p-values for α, v, and m are 1.76×10^{-10}, 2.29×10^{-5}, and 1.91×10^{-12}, respectively, as presented in Table 6. In the present study, the R^2 value of 0.9344 signifies that the model explains 93.44% of the variation in the response variable. This demonstrates that the developed model accurately captures the underlying trend in the experimental observations and establishes a strong correlation between the input parameters and the output response. Furthermore, statistical significance is commonly evaluated at a 95% confidence level, where a variable is considered significant if its p-value is less than 0.05. The p-values obtained for α, v, and m are all substantially lower than 0.05, indicating that each of these variables exerts a statistically significant influence on the response parameter. These results confirm the reliability and robustness of the developed regression model.

http://dx.doi.org/10.21622/RESD.2026.12.1.2100

Table 6: Regression analysis of the observed values for air-injection cases.

Regression Statistics			
Multiple R	0.967		
R Square	0.934		
Adjusted R-Square	0.926		
Standard Error	0.127		
Observations	27		
ANOVA			
	df	**SS**	**F**
Regression	3	5.294	109.293
Residual	23	0.371	
Total	26	5.665	
	Coefficients	**Standard Error**	**P-value**
Intercept	-0.144	0.174	0.417
AOA, α	0.022	0.002	1.7677E-10
Air Flow Rate, v	-0.032	0.006	2.2969E-05
Sediment Concentration, m	0.020	0.001	1.910E-12

To improve the interpretability of the results, error bars are presented in Figure 8 for mean material loss values under non-aerated and aerated conditions. The error bars represent the overall variability associated with repeated measurements and experimental uncertainty.

The plotted results indicate acceptable consistency across the test program. A tendency for larger uncertainty at higher angles of attack is also observed. This behavior is reasonable because stronger hydrodynamic loading and more severe particle interaction can increase sensitivity to small variations in flow structure, specimen exposure, and local sediment distribution. The inclusion of uncertainty bounds strengthens confidence in the reported trends, particularly the consistent reduction in material loss observed with air injection across the investigated operating range.

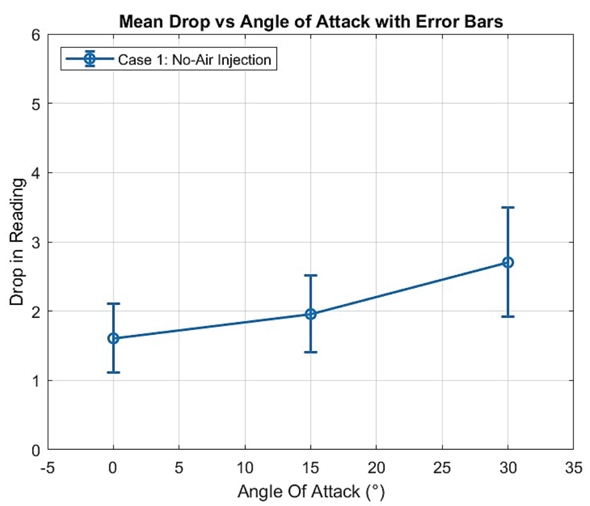

(a)

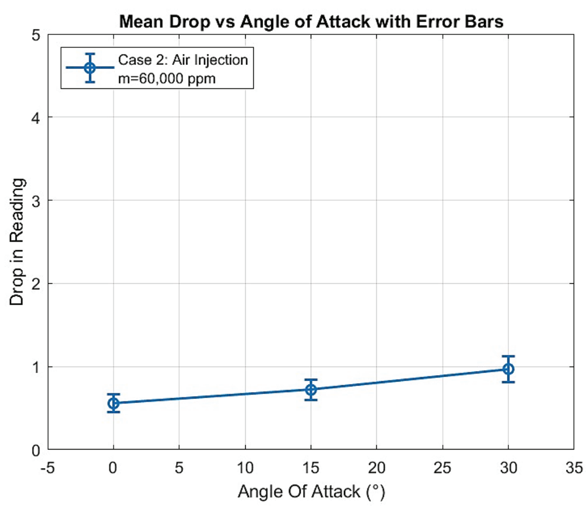

(b)

Volume 12, Issue 1, June 2026 - ISSN 2356-8569
http://dx.doi.org/10.21622/RESD.2026.12.1.2100

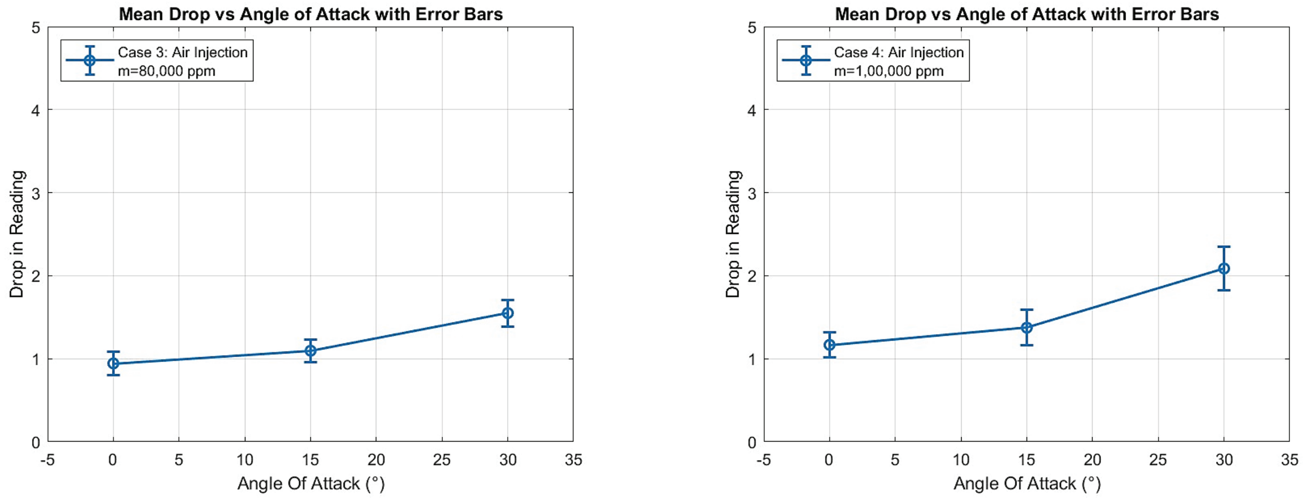

(c) (d)

Figure 8: Error bars for presenting mean drop vs angle of attack for (a) no air-injection condition and for all three sediment conditions, and air-injection conditions for (b) 60,000 ppm, (c) 80,000 ppm, and (d) 1,00,000 ppm of sediment concentration in the water mixture.

VII. Conclusions

The current study investigated the effectiveness of the air-injection technique in reducing the effect of sediment erosion and reducing the material loss from the surfaces of guide vanes. Experimentation was performed for NACA 4412 profile of guide vane samples under pressurized conditions in a rotary disc apparatus replicating the real scenarios of the hydro power plants for different sediment concentrations in the water stream and different angles of attack for the guide vanes, and then compared with the implications of the technique for mitigating sediment erosion.

The mitigation technique of air-injection is applied on the surface of guide vanes and tested for three angles of attack for guide vanes, $\alpha = 0°$, $\alpha = 15°$, and $\alpha = 30°$. These three angles were combined with three values of sediment concentration in the water stream: $m = 60{,}000$ ppm, $m = 80{,}000$ ppm, and $m = 1{,}00{,}000$ ppm. Also, to understand the efficacy of air-injection, guide vane samples are tested for three values of air flow volumes: $v = 15$ Lpm, $v = 20$ Lpm, and $v = 25$ Lpm. The following are the key observations from the experimentation:

- Reduction in material loss is about 32 % to 51% for 1,00,000 ppm of silt concentration for all angles and all air flow volumes.
- Similarly, for 80,000 ppm of silt concentration, reduction in material loss is about 34% to 52%. However, maximum material loss is observed for 60,000 ppm of silt concentration and is about 39% to 58%.
- The higher value of percentage reduction in material loss was observed at the lowest sediment concentration (60,000 ppm). However, the absolute material loss increased with increasing sediment concentration (80,000 ppm and 1,00,000 ppm) under different test conditions.
- Increasing the air flow volume reduces the material loss. Possible reasons are the increased carry-away effect of sediment from the water stream and a more effective envelope of air-injection acting as a shield of air for reducing sediment erosion.
- The erosion patterns shown in the images of the guide vane samples correspond closely with the data presented in the graphs, which compare the material loss from the surface of the samples without and with the air-injection technique.

These findings support the effectiveness of air-injection as a potential mitigation technique for reducing sediment erosion in the components of hydro turbines. However, the reported impact of the air-injection technique used in the current work is attributed entirely to the interaction between the guide vane samples of

NACA 4412 profile fabricated with aluminum alloys under fixed operating conditions To highlight the specific consequences of sediment erosion other influencing parameters such as the power generating efficiency of the hydro turbines, the performance characteristics of the surface coatings on the components of the hydro turbines and additional resistive forces encountered throughout the process of power generation have been either neglected or kept constant for the operating cycles.

Acknowledgements

The authors acknowledge the support received from the Early Career Research Award, Science and Engineering Research Board, Department of Science and Technology, India, under grant no. ECR/2017/002945, as well as the support received under the UPES-SEED grant program from UPES Dehradun.

Conflict of interest

The authors declare that they have no known competing financial interests or personal relationships that could have appeared to influence the work reported in this article.

References

[1] G. Ardizzon, G. Cavazzini, and G. Pavesi, "A new generation of small hydro and pumped-hydro power plants: Advances and future challenges," *Renewable and Sustainable Energy Reviews*, vol. 31, pp. 746–761, Mar. 2014, doi: https://doi.org/10.1016/j.rser.2013.12.043.

[2] U. Dorji and R. Ghomashchi, "Hydro turbine failure mechanisms: An overview," *Engineering Failure Analysis*, vol. 44, pp. 136–147, Sep. 2014, doi: https://doi.org/10.1016/j.engfailanal.2014.04.013.

[3] S. Gautam, H. P. Neopane, N. Acharya, S. Chitrakar, B. S. Thapa, and B. Zhu, "Sediment erosion in low specific speed francis turbines: A case study on effects and causes," *Wear*, vol. 442–443, p. 203152, Feb. 2020, doi: https://doi.org/10.1016/j.wear.2019.203152.

[4] Sailesh Chitrakar, Hari Prasad Neopane, and Ole Gunnar Dahlhaug, "A Review on Sediment Erosion Challenges in Hydraulic Turbines," *InTech eBooks*, Apr. 2018, doi: https://doi.org/10.5772/intechopen.70468.

[5] M. K. Padhy and R. P. Saini, "A review on silt erosion in hydro turbines," *Renewable and Sustainable Energy Reviews*, vol. 12, no. 7, pp. 1974–1987, Sep. 2008, doi: https://doi.org/10.1016/j.rser.2007.01.025.

[6] C. Hauer *et al.*, "State of the art, shortcomings and future challenges for a sustainable sediment management in hydropower: A review," *Renewable and Sustainable Energy Reviews*, vol. 98, pp. 40–55, Dec. 2018, doi: https://doi.org/10.1016/j.rser.2018.08.031.

[7] S. Mishra, S. K. Singal, and D.K. Khatod, "Design of desilting tank for small hydropower projects - A review," *Water and Energy International.*, vol. 68, no. 4, pp. 32–36, Apr. 2011, Available: https://www.researchgate.net/publication/294328024_Design_of_desilting_tank_for_small_hydropower_projects_-_A_review

[8] G. Singh and A. Kumar, "Performance evaluation of desilting basins of small hydropower projects," *ISH Journal of Hydraulic Engineering*, vol. 22, no. 2, pp. 135–141, Jan. 2016, doi: https://doi.org/10.1080/09715010.2015.1094750.

[9] V. Almeida *et al.*, "Approach to sediment monitoring in Hydro Power Plant," *IOP Conference Series: Earth and Environmental Science*, vol. 1079, no. 1, p. 012062, Sep. 2022, doi: https://doi.org/10.1088/1755-1315/1079/1/012062.

[10] A. Kr. Rai and A. Kumar, "Sediment monitoring for hydro-abrasive erosion : A field study from Himalayas, India," *International Journal of Fluid Machinery and Systems*, vol. 10, no. 2, pp. 146–153, Jun. 2017, doi: https://doi.org/10.5293/ijfms.2017.10.2.146.

[11] M. B. Bishwakarma and H. Støle, "Real-time sediment monitoring in hydropower plants," *Journal of Hydraulic Research*, vol. 46, no. 2, pp. 282–288, Mar. 2008, doi: https://doi.org/10.1080/00221686.2008.9521862.

[12] D. Felix, I. Albayrak, and R. M. Boes, "Continuous measurement of suspended sediment concentration: Discussion of four techniques," *Measurement*, vol. 89, pp. 44–47, Jul. 2016, doi: https://doi.org/10.1016/j.measurement.2016.03.066.

[13] R.Kumar, S.Bhandari, and A.Goyal, "Synergistic effect of Al 2 O 3 /TiO 2 reinforcements on slurry erosion performance of nickel-based composite coatings," *Proceedings of the Institution of Mechanical Engineers, Part J: Journal of Engineering Tribology*, vol. 232, no. 8, pp. 974–986, Oct. 2017, doi: https://doi.org/10.1177/1350650117736487.

[14] V. Sharma, M. Kaur, and S. Bhandari, "Slurry erosion performance study of high velocity flame sprayed Ni–Al_2O_3 coating under hydro accelerated conditions," *Materials Research Express*, vol. 6, no. 7, p. 076436, Apr. 2019, doi: https://doi.org/10.1088/2053-1591/ab1927.

[15] G. Prashar, H. Vasudev, and L. Thakur, "Performance of different coating materials against slurry erosion failure in hydrodynamic turbines: A review," *Engineering Failure Analysis*, vol. 115, p. 104622, Sep. 2020, doi: https://doi.org/10.1016/j.engfailanal.2020.104622.

[16] K. R.K., K. M., S. S., and A. K. S., "A pragmatic approach and quantitative assessment of silt erosion characteristics of HVOF and HVAF processed WC-CoCr coatings and 16Cr5Ni steel for hydro turbine applications," *Materials & Design*, vol. 132, pp. 79–95, Oct. 2017, doi: https://doi.org/10.1016/j.matdes.2017.06.046.

[17] S. A. Romo, J. F. Santa, J. E. Giraldo, and A. Toro, "Cavitation and high-velocity slurry erosion resistance of welded Stellite 6 alloy," *Tribology International*, vol. 47, pp. 16–24, Oct. 2011, doi: https://doi.org/10.1016/j.triboint.2011.10.003.

[18] J. F. Santa, L. A. Espitia, J. A. Blanco, S. A. Romo, and A. Toro, "Slurry and cavitation erosion resistance of thermal spray coatings," *Wear*, vol. 267, no. 1–4, pp. 160–167, Jun. 2009, doi: https://doi.org/10.1016/j.wear.2009.01.018.

[19] D. K. Goyal, H. Singh, H. Kumar, and V. Sahni, "Slurry Erosive Wear Evaluation of HVOF-Spray Cr2O3 Coating on Some Turbine Steels," *Journal of Thermal Spray Technology*, vol. 21, no. 5, pp. 838–851, Jun. 2012, doi: https://doi.org/10.1007/s11666-012-9795-5.

[20] Z. Chen and Y.-D. Choi, "Influence of air supply on the performance and internal flow characteristics of a cross flow turbine," *Renewable Energy*, vol. 79, pp. 103–110, Jul. 2015, doi: https://doi.org/10.1016/j.renene.2014.08.024.

[21] K. Kumar and R. P. Saini, "A review on operation and maintenance of hydropower plants," *Sustainable Energy Technologies and Assessments*, vol. 49, no. 101704, p. 101704, Feb. 2022, doi: https://doi.org/10.1016/j.seta.2021.101704.

[22] P. K. Sanjeevaiah and A. Karn, "Enhancement of dissolved oxygen level in the reservoir downstream using air injection techniques in hydroturbines: A review," *Energy Sources, Part A: Recovery, Utilization, and Environmental Effects*, vol. 46, no. 1, pp. 9935–9954, Jul. 2024, doi: https://doi.org/10.1080/15567036.2024.2382325.

[23] R. E. A. Arndt, C. R. Ellis, and S. Paul, "Preliminary investigation of the use of air injection to mitigate cavitation erosion," *Journal of Fluids Engineering, Transactions of the ASME*, vol. 11, no. 3, pp. 498–504, 1995, doi: https://doi.org/10.1115/1.2817290.

[24] A. Karn, “Characterization of Bubbly Flow Systems: A Review,” *International Journal Of Petrochemical Science & Engineering*, vol. 2, no. 6, Jul. 2017, doi: https://doi.org/10.15406/ipcse.2017.02.00053.

[25] A. Karn, R. De, J. Hong, and R. E. A. Arndt, “Closure mechanisms of ventilated supercavities under steady and unsteady flows,” *Journal of Physics: Conference Series*, vol. 656, p. 012145, Dec. 2015, doi: https://doi.org/10.1088/1742-6596/656/1/012145.

[26] A. Karn, S. Shao, R. E. A. Arndt, and J. Hong, “Bubble coalescence and breakup in turbulent bubbly wake of a ventilated hydrofoil,” *Experimental thermal and fluid science*, vol. 70, pp. 397–407, Jan. 2016, doi: https://doi.org/10.1016/j.expthermflusci.2015.10.003.

[27] A. Karn, C. R. Ellis, J. Hong, and Roger, “Investigations into the turbulent bubbly wake of a ventilated hydrofoil: Moving toward improved turbine aeration techniques,” *Experimental Thermal and Fluid Science*, vol. 64, pp. 186–195, Jun. 2015, doi: https://doi.org/10.1016/j.expthermflusci.2014.12.011.

[28] M. S. Sadeq and M. S. Kassim, “Experimental investigation of axial-flow turbine performance using water and oil: effects of rotation speed, blade count, and oil pre-heating,” *Renewable Energy and Sustainable Development*, vol. 11, no. 2, p. 301, Sep. 2025, doi: https://doi.org/10.21622/resd.2025.11.2.1445.

[29] P. Dhiman, A. Bhat, and A. Karn, “The Efficacy of Air Injection in Mitigating Silt Erosion on Hydroturbine Blades: A Computational Study,” *Lecture Notes in Civil Engineering*, pp. 437–444, 2024, doi: https://doi.org/10.1007/978-981-99-6616-5_49.

[30] P. Dhiman, A. Bhat, and A. Karn, “Multiphase Flow Simulations to Explore Novel Technique of Air Injection to Mitigate Silt Erosion in Hydro Turbines,” *Journal of Applied Fluid Mechanics*, vol. 18, no. 2, Feb. 2025, doi: https://doi.org/10.47176/jafm.18.2.2735.

[31] P. Dhiman, V. P. Singh, and A. Karn, “Experimental and computational analysis of air injection as a mitigation technique for silt erosion in hydro turbines,” *Renewable Energy and Sustainable Development*, vol. 10, no. 2, p. 345, Nov. 2024, doi: https://doi.org/10.21622/resd.2024.10.2.1054.

[32] R. Koirala, B. Thapa, H. P. Neopane, and B. Zhu, “A review on flow and sediment erosion in guide vanes of Francis turbines,” *Renewable and Sustainable Energy Reviews*, vol. 75, pp. 1054–1065, Aug. 2017, doi: https://doi.org/10.1016/j.rser.2016.11.085.

[33] R. Koirala, B. Thapa, H. P. Neopane, B. Zhu, and B. Chhetry, “Sediment erosion in guide vanes of Francis turbine: A case study of Kaligandaki Hydropower Plant, Nepal,” *Wear*, vol. 362–363, pp. 53–60, Sep. 2016, doi: https://doi.org/10.1016/j.wear.2016.05.013.

[34] R. Koirala, H. P. Neopane, O. Shrestha, B. Zhu, and B. Thapa, “Selection of guide vane profile for erosion handling in Francis turbines,” *Renewable Energy*, vol. 112, pp. 328–336, Nov. 2017, doi: https://doi.org/10.1016/j.renene.2017.05.033.

[35] E. Quaranta and P. Davies, “Emerging and Innovative Materials for Hydropower Engineering Applications: Turbines, Bearings, Sealing, Dams and Waterways, and Ocean Power,” *Engineering*, vol. 8, Sep. 2021, doi: https://doi.org/10.1016/j.eng.2021.06.025.

[36] O. Shrestha, H. P. Neopane, B. Thapa, Y.-H. Lee, and A. Kapali, “Rotating Disc Apparatus and its application to estimate sediment erosion in Hydro turbines,” *International Journal of Scientific Research in Science and Technology*, pp. 348–358, Dec. 2021, doi: https://doi.org/10.32628/ijsrst218616.

[37] C. Liu, W. Wei, Q. Yan, and N. R. Morgan, “Design of experiments to investigate blade geometric effects on the hydrodynamic performance of torque converters,” *Proceedings of the Institution of Mechanical Engineers Part D Journal of Automobile Engineering*, vol. 233, no. 2, pp. 276–291, Dec. 2017, doi: https://doi.org/10.1177/0954407017742573.

[38] A. Jankovic, G. Chaudhary, and F. Goia, "Designing the design of experiments (DOE) – An investigation on the influence of different factorial designs on the characterization of complex systems," *Energy and Buildings*, vol. 250, no. 111298, p. 111298, Nov. 2021, doi: https://doi.org/10.1016/j.enbuild.2021.111298.

[39] S. J. W. Klein and E. L. B. Fox, "A review of small hydropower performance and cost," *Renewable and Sustainable Energy Reviews*, vol. 169, p. 112898, Nov. 2022, doi: https://doi.org/10.1016/j.rser.2022.112898.

[40] S. Sangal, M. K. Singhal, and R. P. Saini, "Hydro-abrasive erosion in hydro turbines: a review," *International Journal of Green Energy*, vol. 15, no. 4, pp. 232–253, Feb. 2018, doi: https://doi.org/10.1080/15435075.2018.1431546.

[41] N. Shrivastava and A. K. Rai, "Hydro-abrasive erosion in Pelton turbines: Comprehensive review and future outlook," *Renewable and Sustainable Energy Reviews*, vol. 207, p. 114957, Jan. 2025, doi: https://doi.org/10.1016/j.rser.2024.114957.